



Universität Hamburg

DER FORSCHUNG | DER LEHRE | DER BILDUNG

Department of Earth Science System  
Climate, Radiation and Remote Sensing  
Meteorological Institute

## Bachelor's Thesis

# New insight on Earth's longwave radiative feedback from CERES satellite observations

primary supervisor: Prof. Dr. Stefan Bühler  
secondary supervisor: Florian Römer

Leonie Nellesen, 7399948  
Gluckstraße 74c, 22081 Hamburg  
leonie.nellesen@studium.uni-hamburg.de  
B.Sc. Meteorology

Submission:  
Longyearbyen, 19.09.2023



# Abstract

Earth's radiation budget is defined by the equilibrium between incoming shortwave solar radiation, reflected shortwave radiation on earth's surface, and outgoing longwave radiation (OLR). It is essential for climate stability because it determines earth's equilibrium temperature. Increasing greenhouse gases shift this equilibrium to higher temperatures. Water vapor is known as a dominate greenhouse gas. Its concentration increases with increasing temperatures which leads to positive radiative forcing, increasing the equilibrium temperature, resulting in increased amount of water vapor in the atmosphere.

My thesis investigates this growing imbalance, by extending previous research. I analyze the relationship between OLR and two-meter temperature ( $T_s$ ) while considering the impact of water vapor on OLR and the radiative feedback. OLR depends linearly on  $T_s$  which is a consequence of complex interactions between the Stefan-Boltzmann law and the spectral window of water vapor. Theory predicts, that for  $T_s$  higher than a certain threshold, the "super greenhouse effect" occurs and causes OLR to decrease.

To validate this theory, I use data from the CERES satellite product and ERA5 reanalysis and investigate the dependence of OLR, and thus, of the radiative feedback on the column relative humidity (CRH). My analysis identifies regions with high moisture absorption and shows a decrease of the radiative feedback in high CRH areas. Clouds further dampen OLR but the radiative feedback remains humidity-dominated.

Furthermore, I analyze the sudden decrease of OLR around  $T_s = 300$  K, based on previous studies. The decrease is caused by the moist mid-atmosphere of the tropical warm pool.



# Contents

<b>1</b>	<b>Introduction</b>	<b>5</b>
<b>2</b>	<b>Data and Methods</b>	<b>7</b>
2.1	Used data . . . . .	7
2.2	Data processing . . . . .	7
<b>3</b>	<b>Theory and Results</b>	<b>11</b>
3.1	Linearity of OLR and its dependence on CRH . . . . .	11
3.2	All-sky vs. Clear-sky . . . . .	16
3.3	Impact of mid-tropospheric CRH on the feedback . . . . .	20
<b>4</b>	<b>Conclusion and Outlook</b>	<b>25</b>
	<b>Bibliography</b>	<b>29</b>



# 1 Introduction

Greenhouse gases play an important role in influencing earth’s radiation budget, and thus, the two-meter temperature ( $T_s$ ). The radiation budget describes the equilibrium between incoming shortwave solar radiation, reflected shortwave radiation on earth’s surface, and outgoing longwave radiation (OLR). Greenhouse gases absorb the radiation from the surface and reemit at lower temperatures. An increase in greenhouse gases leads to positive radiative forcing and increasing temperatures. A dominant greenhouse gas is water vapor, amount of which is proportional to  $T_s$ . Thus, a sufficient amount of water vapor increases the temperature which leads to even more water vapor in the atmosphere and decreasing OLR. This effect is quantified by the longwave feedback parameter

$$\lambda_{lw} = \frac{dOLR}{dT_s} \quad (1.1)$$

which represents the slope of the linear regression between OLR and  $T_s$ .

Several studies like [Koll and Cronin \[2018\]](#), [McKim et al. \[2021\]](#) and [Feng \[2023\]](#) proved that OLR depends linearly on the near-surface temperature, thus,  $\lambda_{lw}$  is constant. In this thesis, I extend these studies and take the effect of water vapor on the feedback into account.

The linearity between OLR and  $T_s$  arises because of the counteraction between the non-linear Stefan-Boltzmann law and the non-linear effect by the narrowing of the spectral window of water vapor with increasing temperature. The warmer it is the more water vapor can be hosted by the atmosphere. Above a certain threshold the spectral window of water vapor closes, thus, the linearity between OLR and  $T_s$  has to break down. This is known as the super greenhouse effect. It means that the absorption of radiation from the surface due to greenhouse gases is larger than the reemission and the emission from Earth’s surface. This leads to decreasing of OLR.

To perform my analysis, I utilize OLR measurements from the satellite data product CERES and temperature and humidity data from ERA5 reanalysis. I extend the analysis of [Koll and Cronin \[2018\]](#) and [McKim et al. \[2021\]](#) by examining the dependence of OLR on the column relative humidity (CRH). CRH is defined after [Rushley et al. \[2018\]](#) as the relation of, over pressure integrated, specific humidity, and the integrated saturated state of specific humidity.

My main analysis is based on the research question of how CRH affects radiative feedback. In Chapter 3.1 I analyze the positive feedback of water vapor (Formula 1.1) depending on CRH. The higher the temperature the higher the water vapor content in the atmosphere and the higher the absorption of OLR due to the narrowing of the spectral window. Thus, decreasing  $\lambda_{lw}$  is expected as soon as the spectral window of water vapor closes.

To identify moist regions, I bin OLR data by CRH and analyze the effects of moisture on  $\lambda_{lw}$ . Within these bins, I assume constant CRH which does not fit observations but makes

## 1 Introduction

it comparable to models which will not be discussed further in this thesis.

Another aspect that impacts OLR is clouds (Chapter 3.2). I compare clear-sky and all-sky data like [McKim et al. \[2021\]](#) and analyze how clouds affect OLR and the radiative feedback.

Furthermore, based on a talk by [Feng \[2023\]](#), I investigate the sudden decrease of OLR around  $T_s = 300$  K in Chapter 3.3. The moist tropical warm pool causes the decrease of OLR. [Feng \[2023\]](#) found, that this feature is dominated by the mid-tropospheric CRH. I analyze the effect of mid-tropospheric CRH on the radiative feedback for the whole  $T_s$  and for  $T_s > 290$  K.



## 2 Data and Methods

### 2.1 Used data

My analysis is based on OLR data from the satellite project "Clouds and the Earth's Radiant Energy System" [CERES \[2022\]](#) and temperature and humidity data from the fifth generation of European Centre for Medium-Range Weather Forecasts reanalysis [ERA5 \[2022\]](#).

CERES is a project of NASA. It consists of seven instruments on five different satellites. The project aims to produce a time series of Earth's global radiation budget from March 2000 until today. From this product, I use monthly mean OLR measurements of a sun-synchronous polar orbiting satellite with a spatial resolution of a  $1^\circ \times 1^\circ$  latitude-longitude grid.

ERA5 covers a time series from 1940 until today and uses a  $0.25^\circ \times 0.25^\circ$  latitude-longitude grid. I use monthly mean two-meter temperature data and specific humidity data on the pressure levels 1000 hPa, 850 hPa, 700 hPa, 500 hPa, 400 hPa, and 300 hPa.

To combine both datasets I have to regrid the spatial resolution of ERA5 to a  $1^\circ \times 1^\circ$  latitude-longitude grid. I do that by only using data points with the same coordinates. The time series starts on March 2000 until December 2022.

### 2.2 Data processing

The humidity variable I use for my analysis is CRH. I use this humidity variable as it weighs the different atmospheric layers by taking pressure into account. CRH is similar to relative humidity as it describes the relative humidity within a column by taking the ratio of integrated water vapor (IWV) and saturated integrated water vapor (IWVS)

$$\text{CRH} = \frac{\text{IWV}}{\text{IWVS}}. \quad (2.1)$$

For my calculation, I use the python package [Typhon \[2023\]](#) which is a toolbox with functions for atmospheric radiative research developed by the working group of Stefan Bühler. To calculate CRH, I need to calculate the integrated water vapor (IWV) using

$$\text{IWV} = -\frac{1}{g} \int_{p_l}^{p_u} q(p) dp, \quad (2.2)$$

with the gravitational constant  $g = 9.81 \text{ ms}^{-2}$ , the lower pressure boundary  $p_l$ , and the upper pressure boundary  $p_u$ . The function uses the volume mixing ratio ( $x$ ) to calculate the specific humidity

$$q = \frac{x}{(1-x)\frac{M_d}{M_w} + x}, \quad (2.3)$$

which is needed in Equation 2.2. As I initially need  $x$  as an input to use the existing Function 2.2 in [Typhon \[2023\]](#) I use

$$x = \frac{q}{(1-q)\frac{M_w}{M_d} + q}, \quad (2.4)$$

with the molar mass for dry air  $M_d = 28.9647 \text{ g mol}^{-1}$  and the molar mass for moist air  $M_w = 18.01528 \text{ g mol}^{-1}$  to convert the given  $q$  in the ERA5 data into  $x$ .

To get IWVS I convert the, in ERA5 given, temperature  $T$  into saturated water vapor pressure  $e_s$  using a Formula by [Murphy and Koop \[2005\]](#) which is implemented in [Typhon \[2023\]](#).

I then calculate the saturated specific humidity  $q_s$  with saturated water vapor pressure  $e_s$  and pressure  $p$  to derive saturated specific humidity

$$q_s = \frac{0.622 \cdot e_s}{p - 0.378 \cdot e_s}. \quad (2.5)$$

With  $q_s$  I have the same starting point as for the derivation of IWV using  $q$ . I repeat Formula 2.2, Formula 2.3 and Formula 2.4 to calculate IWVS using  $q_s$ . Lastly, I divide IWV by IWVS to get CRH (Formula 2.1).

I use two different variants of CRH as I analyze the effects of the mid-troposphere in Chapter 3.3. The first variant uses near-surface pressure ( $p_l = 1000 \text{ hPa}$ ) and  $p_u = 300 \text{ hPa}$  as integrating limits in Formula 2.2. Later, it will be referred to as  $\text{CRH}_{1000}$ . The second variant uses pressure from the middle troposphere ( $p_l = 700 \text{ hPa}$ ) to  $p_u = 300 \text{ hPa}$  as integrating limits. Later, it will be referred to as  $\text{CRH}_{700}$ .

During my thesis, I implemented a new function in [Typhon \[2023\]](#) to simplify the derivation of CRH. I combined the previous equations into one function in [Typhon \[2023\]](#). The function will be in the next release of [Typhon \[2023\]](#).

To analyze the radiative feedback with emphasis on humidity, I bin OLR and  $T_s$  data by CRH. The bin width is 10 percent points, starting from 10% to 100%, thus, dry and oversaturated parts of the atmosphere are neglected as there are not many data points.

For a better comparison between CERES and ERA5, I calculate clear-sky humidity data of ERA5  $q_{cs}$ . Because CERES data is available as clear-sky and all-sky and ERA5 data does not distinguish between clear-sky and all-sky. Therefore, I use the cloud fraction  $f_c$  and assume that every grid cell (every value) consists of a cloud-free part and a cloudy part. The actual value of a variable is determined by the sum of both values (Equation 2.6). Equation 2.7 provides the clear-sky part of  $q$  which is  $q_{cs}$

$$q = q_s \cdot f_c + q_{cs} \cdot (1 - f_c) \quad (2.6)$$

$$q_{cs} = \frac{q - q_s \cdot f_c}{1 - f_c}. \quad (2.7)$$

I use the definitions of CRH and the clear-sky calculations of ERA5 in the following

chapter to analyze their effects on the radiative feedback and compare my results of [Koll and Cronin \[2018\]](#), [McKim et al. \[2021\]](#) and [Feng \[2023\]](#).



# 3 Theory and Results

## 3.1 Linearity of OLR and its dependence on CRH

Multiple studies like [McKim et al. \[2021\]](#), [Feng \[2023\]](#), and [Koll and Cronin \[2018\]](#) found that earth's OLR depends linearly on the  $T_s$  for a temperature range between 220 K and 280 K. Thus, the radiative feedback parameter  $\lambda_{lw}$  (Equation 1.1) is to the first order independent of temperature, and the radiative feedback remains the same across all temperatures. The linearity arises due to the counteraction between the Stefan-Boltzmann law

$$E_b = \sigma T^4, \tag{3.1}$$

using the Stefan-Boltzmann constant  $\sigma = 5.67 \cdot 10^{-8} \text{ Wm}^{-2}\text{K}^{-4}$ , the temperature  $T$ , and the black body irradiance ( $E_b$ ), and the absorption by water vapor. Both phenomena are strongly nonlinear. The emitted  $E_b$  increases rapidly with temperature, hence, it leads to greater OLR. The OLR increase is balanced by the narrowing of the spectral window of water vapor due to rising temperature because water vapor acts as an absorber and its concentration increases with temperature. Water vapor is a greenhouse gas because it absorbs radiation from Earth's surface and re-emits at colder temperatures. Thus, OLR is damped by water vapor in the atmosphere as it weakens Earth's radiation from the surface [Koll and Cronin \[2018\]](#) state that there are two mechanisms, line absorption, and self-continuum absorption, which cause water vapor to absorb infrared radiation. Absorption by water vapor is proportional to the power of four of its concentration which is highly dependent on the temperature. Thus, the higher the temperature, the more absorption by water vapor takes place and the smaller the spectral window of water vapor (Figure 3.1). The narrowing of water vapor's spectral window leads to the assumption that the linearity between OLR and  $T_s$  has to break down for temperatures above a certain threshold because the spectral window of water vapor closes completely. [Koll and Cronin \[2018\]](#) found, that at  $T_s > 320 \text{ K}$  continuum absorption becomes optically thick and the spectral window of water vapor closes. They used relative humidity (RH) = 100%. The closing of the spectral window of water vapor is also found by [McKim et al. \[2021\]](#) (Figure 3.2), they distinguished between temperatures at 275 K, and at 300 K and show that the spectral window of water vapor closes more rapidly with increasing RH for high temperatures. Hence, they stated that humidity plays an important role in earth's radiative feedback (Figure 3.3). It is clear to see that the radiative feedback decreases more significantly with CRH for higher temperatures.

This motivated me to analyze the feedback not only regarding the temperature but regarding CRH bins.

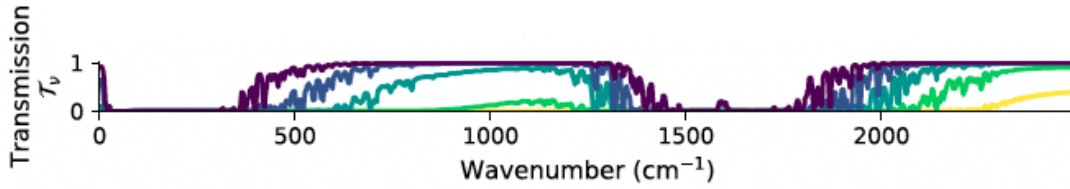


Figure 3.1: Transmissivity of water vapor for the temperatures 320 K (yellow), 300 K (light green), 280 K (turquoise), 260 K (blue) and 240 K (purple) and with RH = 100%. The figure is from [Koll and Cronin \[2018\]](#) with kind permission by Proceedings of the National Academy of Sciences.

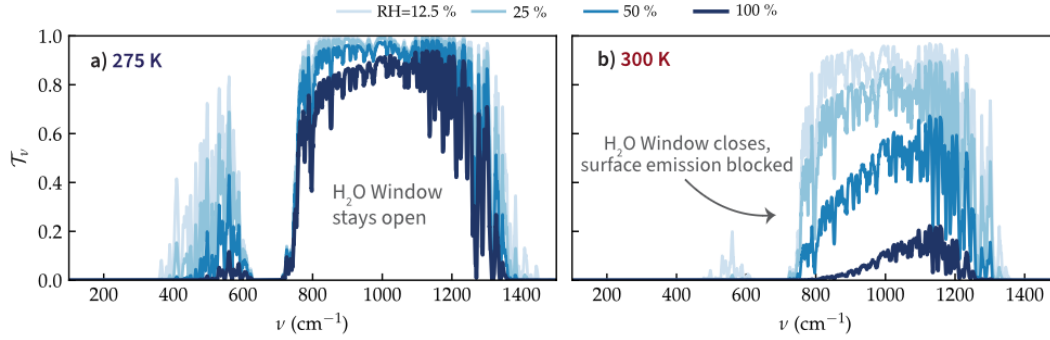


Figure 3.2: The left panel shows the transmissivity of water vapor at 275 K. The right panel shows the transmissivity at 300 K. RH is indicated by the colors. The figure is from [McKim et al. \[2021\]](#) with kind permission by Geophysical Research Letters.

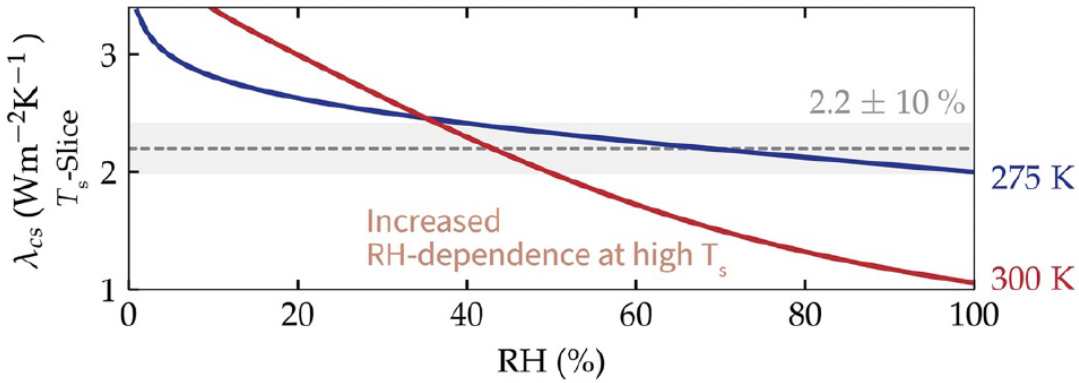


Figure 3.3: Dependence of the radiative feedback on CRH and  $T_s$ . The x-axis is CRH (RH is a short form for CRH). The figure is from [McKim et al. \[2021\]](#) with kind permission by Geophysical Research Letters.

I recreate a figure of [Koll and Cronin \[2018\]](#) which shows the linearity between OLR and  $T_s$  (Figure 3.4). My results provide the radiative feedback parameter  $\lambda_{lw} = 2.194 \text{ W m}^{-2} \text{ K}^{-1}$  (Equation 1.1), while [Koll and Cronin \[2018\]](#) found  $\lambda_{lw} = 2.218 \text{ W m}^{-2} \text{ K}^{-1}$ . The deviation can be explained by the usage of different data sets. [Koll and Cronin \[2018\]](#) used National Centers for Environmental Prediction (NCEP) reanalysis data and I use ERA5 data. Note that in Figure 3.4 a few data points are higher than the black body radiation. This can be explained by my usage of  $T_s$ . If  $T_s$  is lower than the actual surface temperature it seems like the emission is stronger than the black body emission but this is only because

the actual emission temperature is higher than  $T_s$ .

In this chapter and the next chapter, I write CRH instead of  $CRH_{1000}$  because the difference between  $CRH_{1000}$  and  $CRH_{700}$  is not discussed in these chapters.

I weigh the data with their latitude in order to reduce the impact of the poles as the data point density increases with latitude. This weighting does not affect the feedback. In order to take humidity into account, I bin the data by CRH as mentioned in Chapter 2.2 in bins with a width of 10 percent points and without  $CRH < 10\%$  and  $CRH > 100\%$ .

The results of my analysis fit the expectations, that the radiative feedback decreases with increasing CRH. The OLR dependence on  $T_s$  for all-sky ERA5 data and clear-sky CERES data binned with CRH can be seen in Figure 3.5. I mix all-sky ERA5 data with clear-sky CERES data because it does not have a crucial impact on OLR and the feedback. I discuss this in Chapter 3.2. The black line visualizes the mean unbinned feedback  $\lambda_{lw} = 2.194 \text{ W m}^{-2} \text{ K}^{-1}$ , and the light blue lines visualize the feedback of every bin. The dark blue line shows the mean OLR for every  $T_s$  bin.

The decrease of feedback with CRH and the comparison to the mean feedback can be seen in Figure 3.6. Feedback for  $CRH < 40\%$  is higher than the mean feedback because there is less humidity that damps OLR at high temperatures. For  $CRH > 40\%$  the feedback decreases almost linearly to a minimum of  $1.602 \text{ W m}^{-2} \text{ K}^{-1}$  for  $CRH > 90\%$ . An explanation that the decrease is not monotone might be that I use all-sky ERA5 data which affects the CRH and thus the binning by CRH. Only the feedback with the highest CRH deviates more than 10% from the mean feedback. Compared to McKim et al. [2021] (Figure 3.3) all binned feedbacks are relatively close to the mean feedback. In Figure 3.6 the feedbacks with low CRH deviate only very little from the mean feedback while in the results of McKim et al. [2021] (Figure 3.3) for both temperature ranges the feedback with low CRH deviates up to more than 50%. For high CRH the deviation is only for  $T_s = 275 \text{ K}$  up to 50%, while in my results the deviation for the highest CRH bin is 27%. The differences in the results can be caused by the usage of different datasets. McKim et al. [2021] used a 1D model and I use ERA5 combined with satellite data from CERES. Model data is idealized and provide much smoother results than measurements.

The striking difference in my results between the two feedbacks with the highest CRH might represent the super greenhouse effect, which is a scenario with continuum absorption and thus a closed spectral window of water vapor. In Figure 3.5 this can be seen as well by comparing the steepness of the light blue and the black line. However, it should be kept in mind, that the temperature range for the bin with the highest CRH is a lot smaller than for the other bins. This might bias the linear regression as well.

Another noticeable aspect is that the OLR is higher than the average in dry bins, as expected because there is less water vapor to dampen the radiation. Conversely, in moist bins, the OLR is below the average, thus,  $\lambda_{lw}$  decreases. This effect is most visible at high temperatures.

Furthermore, it can be seen in Figure 3.5 that the  $T_s$  range and the OLR range decrease for higher CRH because there are no cold and no warm areas with very high CRH. The warmest regions are deserts which have low CRH, thus, they are not visible in the moistest

bin. On the other hand, the coldest areas like Antarctica are also not visible in the moistest bin because even though the temperatures are very low it is still arid. It can be also seen that most histograms show a gap of data points for  $T_s$  and OLR which separates the histogram in two patches. This gap moves from lower to warmer  $T_s$  for higher CRH but I do not find an explanation for that effect.

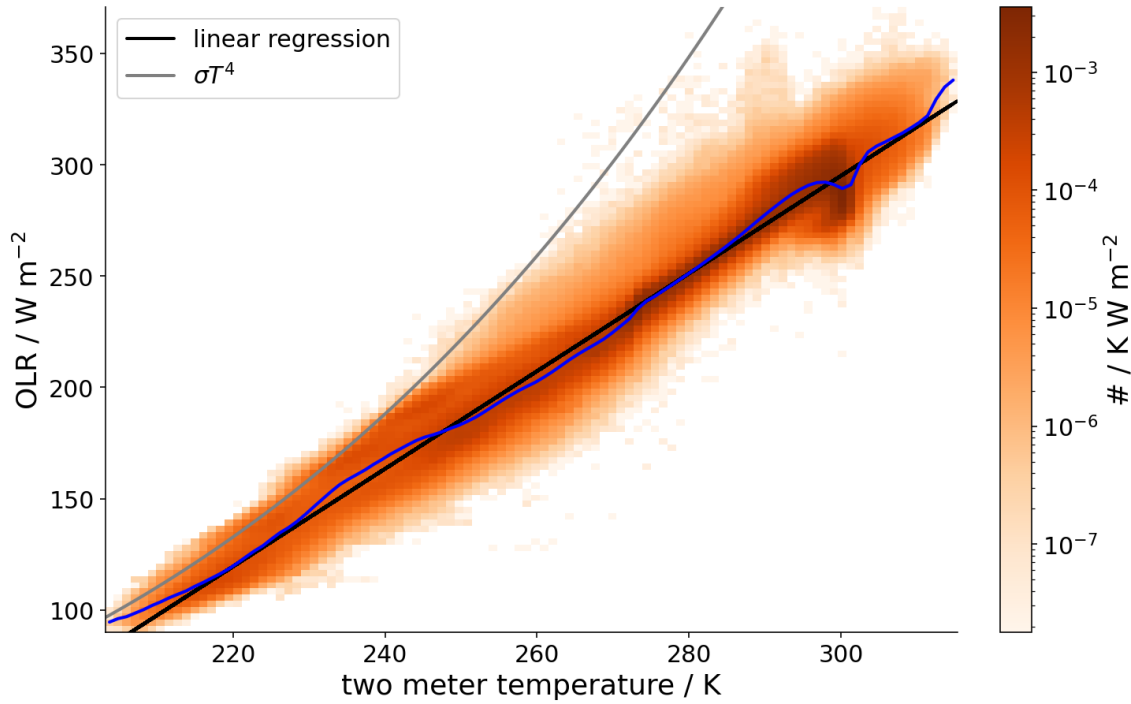


Figure 3.4: This plot is a recreation of a plot by [Koll and Cronin \[2018\]](#). Earth's OLR dependence on  $T_s$  is visible. The grey line is the Stefan-Boltzmann and represents the black body emission. The black line represents the mean feedback and the dark blue line indicates the mean OLR value for every  $T_s$  bin.



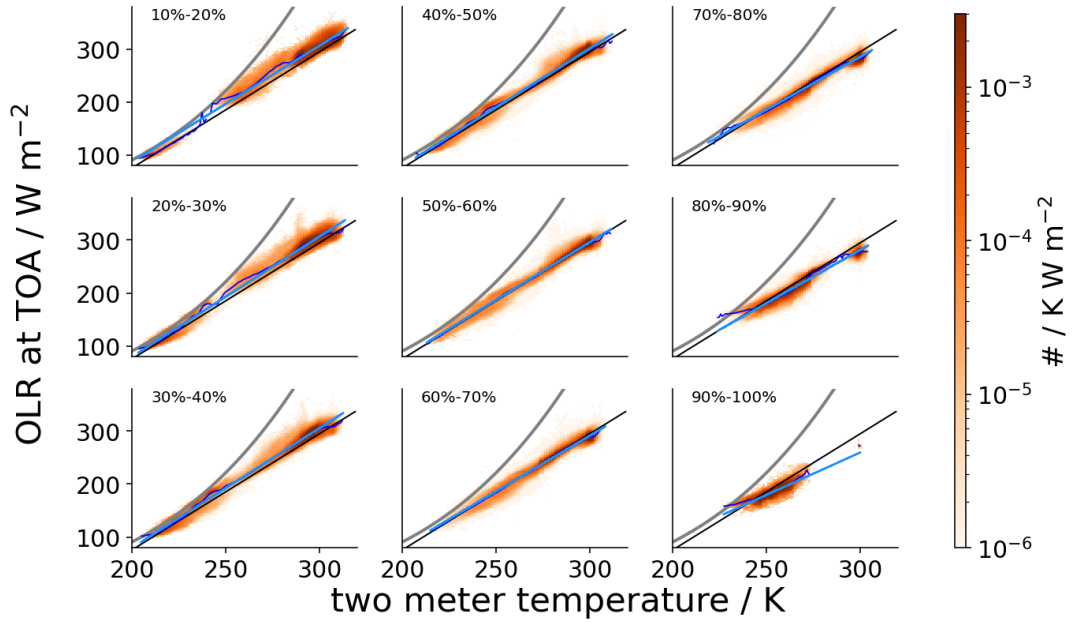


Figure 3.5: OLR (clear-sky CERES) dependence on  $T_s$  (all-sky ERA5) binned by CRH. The grey line indicates the Stefan-Boltzmann law (Equation 3.1), the black line indicates the mean radiative feedback ( $\lambda_{lw} = 2.194 \text{ W m}^{-2} \text{ K}^{-1}$ ), the light blue line indicates the feedback of every bin and the dark blue line indicates the mean OLR value for every  $T_s$  bin.

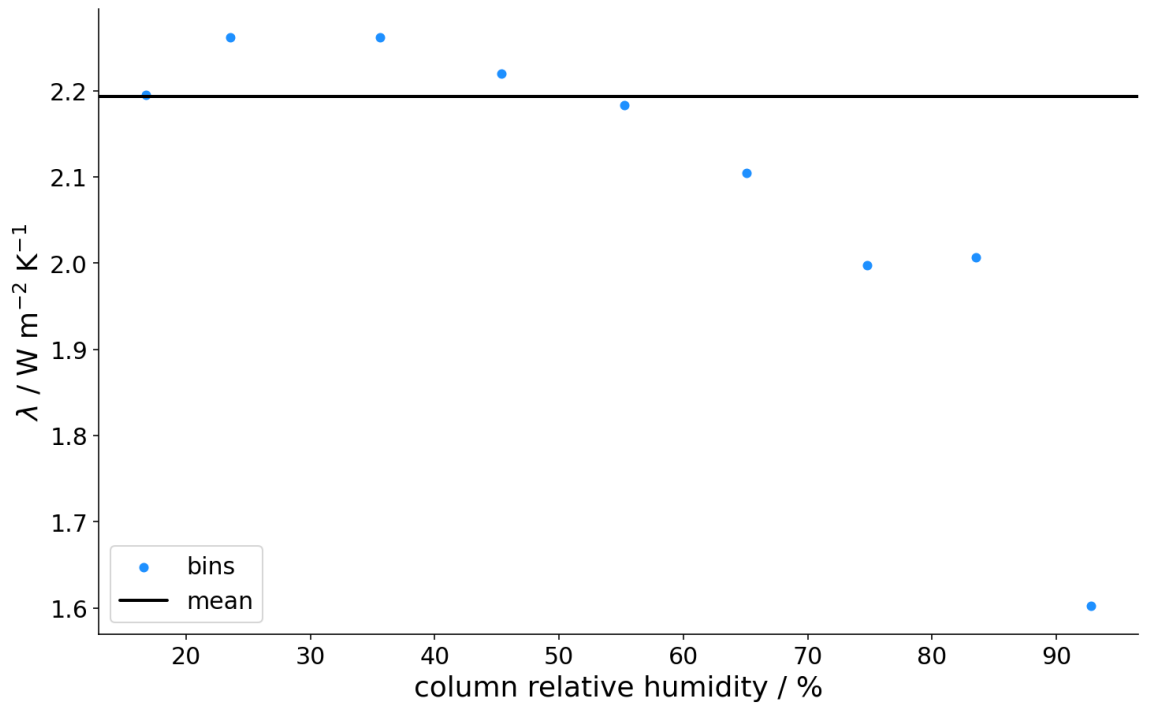


Figure 3.6: Radiative feedback parameter depending on CRH. The black line is the mean unbinned feedback, which is the slope of the black line in Figure 3.4 and 3.5. The light blue dots are the binned feedbacks which are the slopes of the light blue lines in Figure 3.5.

### 3.2 All-sky vs. Clear-sky

As I already stated  $T_s$  is not the only parameter that controls  $\lambda_{lw}$ , I examine the impact of clouds and compare all-sky data with clear-sky data. This discussion is based on [McKim et al. \[2021\]](#) as they studied the impact of clouds on longwave emission and found that clouds have a weakening impact on the radiative feedback. However, the feedback is still impacted by CRH.

In Chapter 3.1 I use all-sky ERA5 data, and clear-sky CERES data. With the aim of a better comparison, I use Formula 2.7 to calculate the clear-sky part of specific humidity  $q_{cs}$ . This allows me to compare the combinations of all-sky ERA5 data with all-sky CERES data and clear-sky ERA5 data with clear-sky CERES data. My calculation for clear-sky OLR ( $OLR_{cs}$ ) is similar to [McKim et al. \[2021\]](#). The only difference is that they only used high clouds for the impact on longwave emission and neglected the impact of low clouds. [McKim et al. \[2021\]](#) also verified their calculation of all-sky OLR ( $OLR_{as}$ ) by comparing it with all-sky reanalysis data, which gives me confidence that my calculations are realistic enough because there are only slight underestimations in the tropics and slight overestimations everywhere else compared to [McKim et al. \[2021\]](#).

Nevertheless, I verify my clear-sky calculation for ERA5 using Figure 3.7. The plot shows

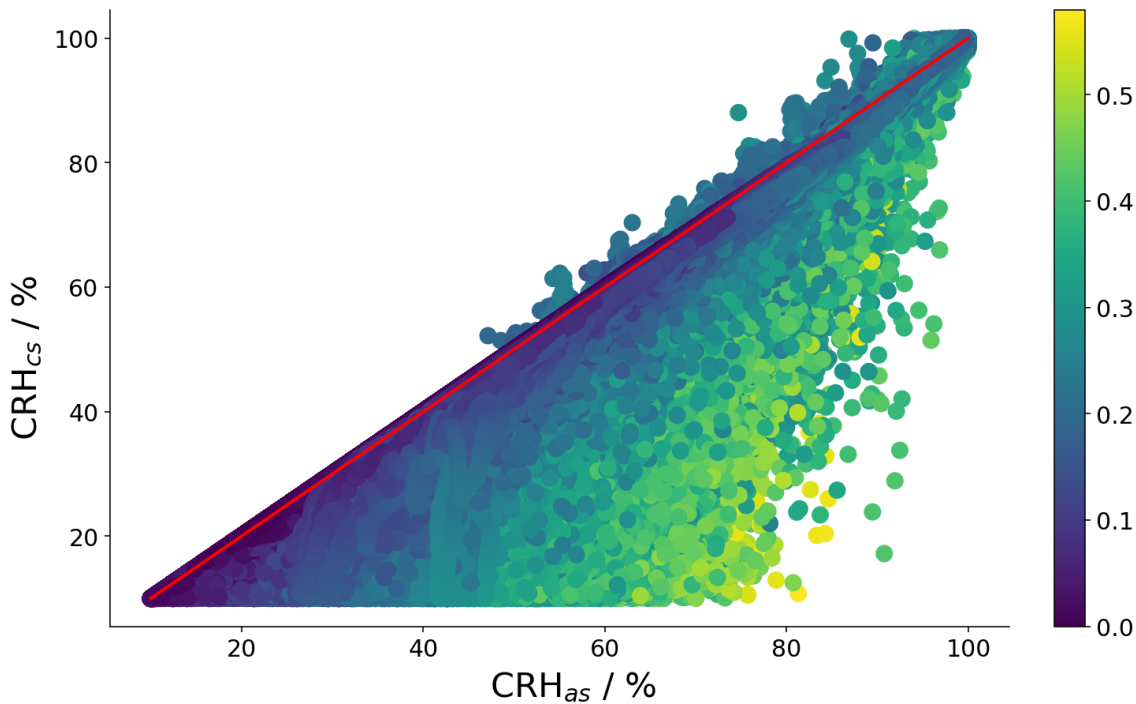


Figure 3.7:  $CRH_{cs}$  dependence on  $CRH_{as}$ . The red line visualizes  $CRH_{cs}=CRH_{as}$ . The color indicates the mean cloud fraction of a column.

that  $CRH_{cs}$  is mostly lower than the  $CRH_{as}$  because clouds have  $RH = 100\%$ . Thus, if  $CRH_{cs}$  is smaller than  $CRH_{as}$  there have to be clouds. However, there are a few exceptions, with  $CRH_{cs} > CRH_{as}$  for  $CRH_{as} > 40\%$ , that might be explained by the poor vertical resolution. Low  $CRH_{cs}$  have a wide range of related  $CRH_{as}$ . The range gets smaller for higher  $CRH_{cs}$  because  $CRH_{as}$  can not be higher than 100%. The  $f_c$  is low if  $CRH_{cs} = CRH_{as}$  because if there is no cloud then there is no difference between clear-sky and all-sky. Moreover the higher the difference between  $CRH_{cs}$  and  $CRH_{as}$ , the higher

the  $f_c$ .

I start with comparing clear-sky ERA5 data with all-sky ERA5 data combined with clear-sky CERES data (Figure 3.8 and Figure 3.9 (green and red)). Figure 3.8 is very similar to Figure 3.5. The difference between clear-sky ERA5 data and all-sky ERA5 data can be seen in Figure 3.9 (green and red). Less humidity slightly impacts the CRH, and thus the feedback. The mean unbinned feedback  $\lambda_{lw} = 2.203 \text{ W m}^{-2} \text{ K}^{-1}$  of clear-sky ERA5 data is higher than using all-sky ERA5 data ( $\lambda_{lw} = 2.194 \text{ W m}^{-2} \text{ K}^{-1}$ ). The binned clear-sky ERA5 feedbacks are not necessarily higher than the all-sky ERA5 feedbacks even though clouds in all-sky ERA5 data affect CRH (Figure 3.9). It is noticeable that the feedback decreases more smoothly using clear-sky ERA5 data than for using all-sky ERA5 data. The difference between all-sky and clear-sky ERA5 data is small because it only affects  $q$  and not OLR since OLR is a satellite product from CERES.

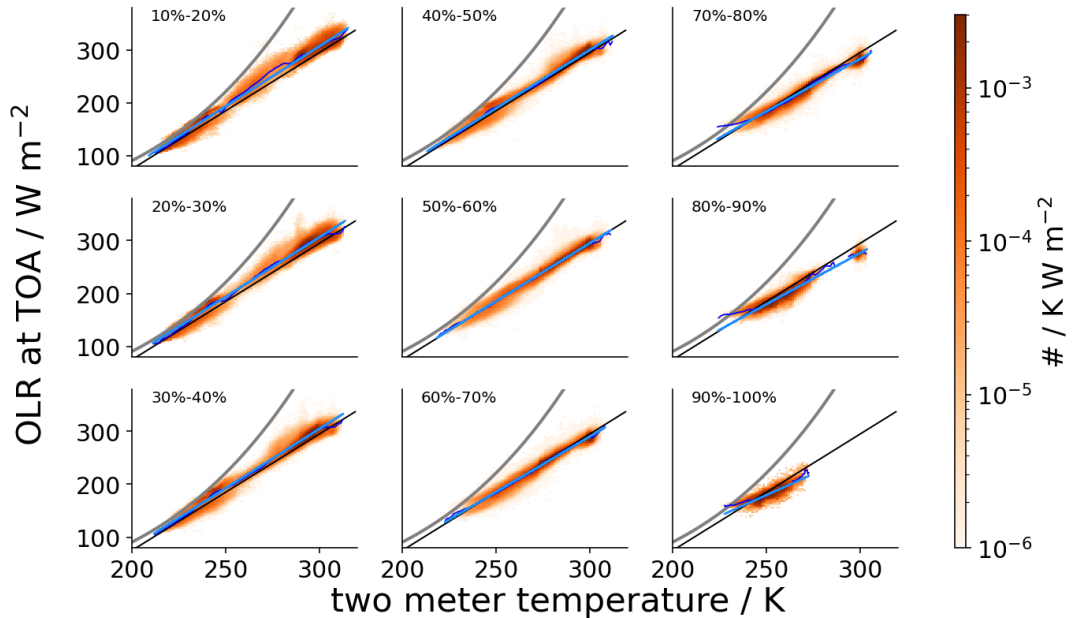


Figure 3.8: OLR (clear-sky CERES) dependence on  $T_s$  (clear-sky ERA5) binned by CRH. The grey line indicates the Stefan-Boltzmann law (Equation 3.1), the black line indicates the mean radiative feedback ( $\lambda_{lw} = 2.203 \text{ W m}^{-2} \text{ K}^{-1}$ ), the light blue line indicates the feedback of every bin and the thin dark blue line indicates the mean OLR value for every  $T_s$  bin.

For the comparison between all-sky and clear-sky CERES data, I combine both data sets with all-sky ERA5 data to isolate the differences in CERES data (red and blue in Figure 3.9). I also compare my results to McKim et al. [2021].

The all-sky radiative feedback (Figure 3.9 (light blue)) is generally lower than the clear-sky feedback (red). This is the result of clouds as they dampen OLR by absorption and by re-emission at lower temperatures. The mean unbinned all-sky feedback  $\lambda_{lw} = 1.746 \text{ W m}^{-2} \text{ K}^{-1}$  is  $0.46 \text{ W m}^{-2} \text{ K}^{-1}$  lower than the mean unbinned clear-sky feedback.  $\lambda_{lw}$  behaving like that not only fits my expectations, it is also seen by McKim et al. [2021]. The all-sky feedback is around  $0.5 \text{ W m}^{-2} \text{ K}^{-1}$  lower than the clear-sky feedback. In my

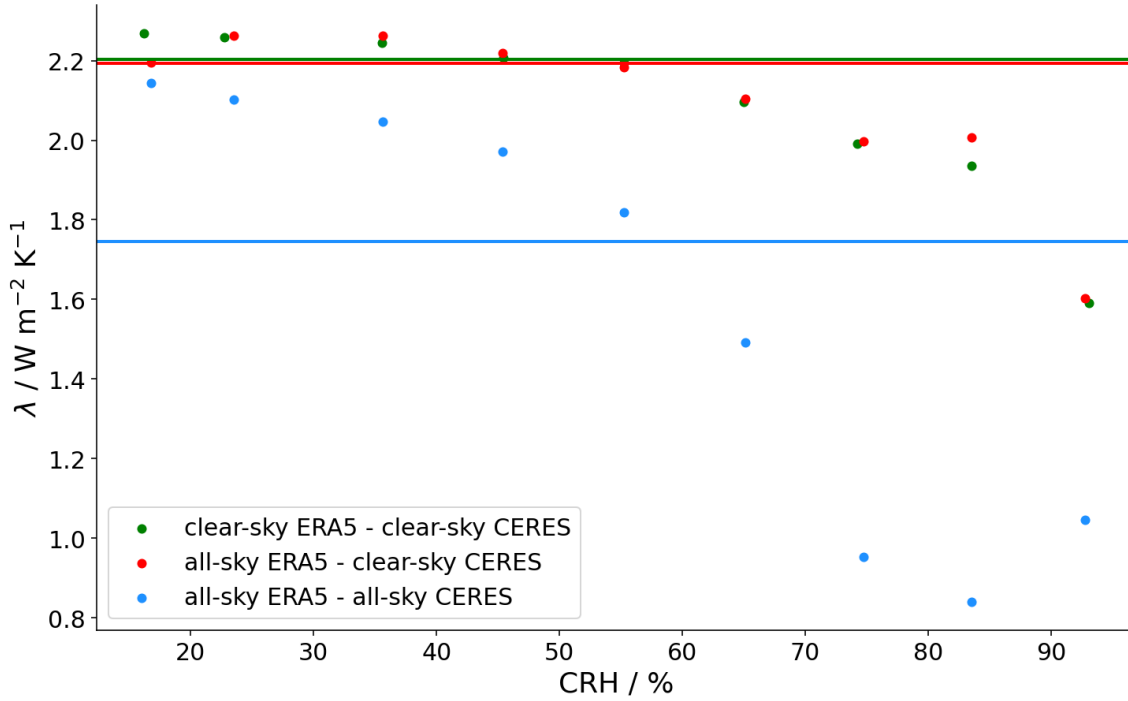


Figure 3.9: Feedback of clear-sky CERES data and all-sky ERA5 data (red), clear-sky CERES data and clear-sky ERA5 data (green), and all-sky CERES data and all-sky ERA5 data (light blue). The solid lines represent the mean unbinned feedback and the dots represent the binned feedback.

results, the difference for low CRH is not that striking but the all-sky feedback decreases much faster with higher CRH than the clear-sky feedback because clouds are more likely to be in areas with high CRH. It decreases to  $0.84 \text{ W m}^{-2} \text{ K}^{-1}$  for the second to last CRH bin and increases again in the last CRH bin. In the clear-sky feedback the second to last bin is at  $1.94 \text{ W m}^{-2} \text{ K}^{-1}$ , and thus more than twice as high. The increase of  $\lambda_{lw}$  in the last bin has to be caused by clouds because it does not happen for clear-sky CERES data. This might be due to a smaller temperature difference between cloud top and surface compared to regions with lower CRH.

Comparing Figure 3.10 and Figure 3.5 it is clear to see, that the lower boundary of the all-sky OLR in general is lower than the lower boundary of clear-sky OLR because clouds dampen OLR. The upper boundary does not change between all-sky and clear-sky. The range of OLR increases for high  $T_s$  bins. In these  $T_s$  bins the lower parts of OLR represent cloudy parts while the upper part of OLR is dominated by clear-sky OLR.

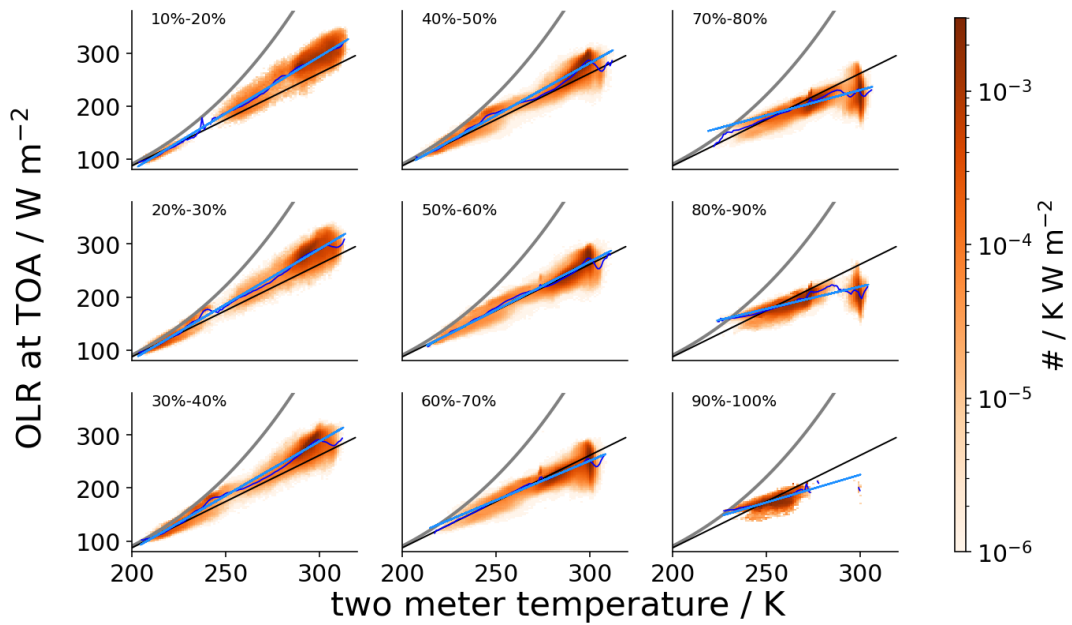


Figure 3.10: OLR (all-sky CERES) dependence on  $T_s$  (all-sky ERA5) binned by CRH. The grey line indicates the Stefan-Boltzmann law (Equation 3.1), the black line indicates the mean radiative feedback ( $\lambda_{lw} = 1.746 \text{ W m}^{-2} \text{ K}^{-1}$ ), the light blue line indicates the feedback of every bin and the dark blue line indicates the mean OLR value for every  $T_s$  bin.

### 3.3 Impact of mid-tropospheric CRH on the feedback

Theory predicts that the overall linearity of  $\lambda_{lw}$  has to break down for  $T_s$  above a certain threshold as the spectral window of water vapor closes. Figure 3.4 shows an increase of OLR for  $T_s < 298$  K and a sudden decrease of OLR for  $T_s > 298$  K. This leads to the assumption that there has to be another impacting factor on the feedback besides  $T_s$  and cloud cover.

Feng [2023] found that the mid-tropospheric CRH in the subtropics and the tropics play an important role in the sudden decrease of OLR around 300 K. A tropical circulation causes this feature. Warm and moist air ascends above the tropical warm pool near the equator and descends above the drier and colder subtropical ocean. Due to the moisture above the equator, the emission temperature is lower compared to drier areas. The emission temperature is the temperature at which the atmosphere emits longwave radiation. This is the point where the opacity equals one looking from space. Since the atmosphere above the equator is very moist the emission happens at higher altitudes, thus, at lower temperatures which decreases OLR. This can be seen in the sudden decrease of OLR for  $T_s > 298$  K in Figure 3.4. The emission temperature of water vapor above the drier subtropical ocean is higher because there is less humidity. Thus, OLR increases which can be seen in Figure 3.4 for  $280 \text{ K} < T_s < 298 \text{ K}$ .

Feng [2023] analyzed the contribution to OLR of the different layers in the atmosphere and found that the bump around 300 K is mainly caused by layers between 750 hPa to 250 hPa. In her analysis, this layer shows a low transmissivity for  $T_s < 302$  K (near the equator) because the mid-troposphere is very moist and contributes less than dry areas to OLR as it gets damped. For  $T_s < 302$  K, north and south of the equator, the mid-troposphere is very dry, thus, all layers in the mid-troposphere contribute equally to OLR as the transmissivity is very high. This effect can be seen in my analysis around  $T_s = 298$  K. The dark blue line in Figure 3.4 indicates the feedback for every  $T_s$  bin. The decrease of OLR for  $T_s > 298$  K happens for moist areas in the mid-troposphere while the increase for  $T_s < 298$  K happens in areas with a dry mid-troposphere.

The global distribution of CRH can be seen in Figure 4.1 and Figure 4.2 in the Appendix. I use the results of Feng [2023] as a starting point for my investigation of whether mid-tropospheric CRH has an impact on the feedback or not.

To do so, I firstly analyze if the decrease of OLR is visible when I use  $CRH_{700}$  for the binning (Figure 3.11) instead of  $CRH_{1000}$  (Figure 3.5).

I expected that the bump around 300 K in Figure 3.4 is more visible in warm and moist areas of the mid-troposphere (Figure 3.11) than warm and moist parts of the whole troposphere (Figure 3.5) due to the change of emission temperature which is dominated by mid-tropospheric CRH. My results are not as clear as expected. In Figure 3.5 the bump is weakly noticeable for all panels except the moistest because there are only very few data points for  $T_s > 280$  K. The sudden decrease of OLR around 300 K is more prominent in Figure 3.11 and it strengthens with increasing  $CRH_{700}$ . This might be explained by the poor vertical resolution of the ERA5 data I have used.

Since Feng [2023] found that the mid-tropospheric CRH is responsible for the decrease of OLR around 300 K it might have an effect on the feedback.

Figure 3.12 compares the radiative feedback binned by  $\text{CRH}_{1000}$  (red) with the radiative feedback binned by  $\text{CRH}_{700}$  (blue). The feedback binned by  $\text{CRH}_{1000}$  decreases with CRH while the feedback binned by  $\text{CRH}_{700}$  shows a decrease for dry bins. For  $\text{CRH}_{700} > 30\%$  it is nearly constant and fluctuates around  $\lambda_{lw} = 1.97 \text{ W m}^{-2}$ . Thus, even though, mid-tropospheric CRH has an effect on the sudden decrease of OLR around 300 K, it does not have an effect on the mean feedback. Note that the OLR and temperature ranges of the  $\text{CRH}_{700}$  bins in Figure 3.11 differ from the ranges of the  $\text{CRH}_{1000}$  bins in Figure 3.5. The  $T_s$  range determines the feedback. Thus, Figure 3.11 is hardly comparable to Figure 3.5 due to the change of the binning. Hence, it is convenient to compare the binning of the different CRH definitions for the same  $T_s$  range which is approximately  $T_s > 290 \text{ K}$ . I use this temperature range because, as McKim et al. [2021] found, the spectral window of water vapor closes for temperatures higher 300 K (Figure 3.2).  $T_s > 290 \text{ K}$  already shows the expected effect and  $T_s > 300 \text{ K}$  does not have enough data points.

The effect of  $T_s > 290 \text{ K}$  on the feedback is summarized in Figure 3.13, which is my main finding of this chapter. It is clear to see, that rising mid-tropospheric CRH has a decreasing impact on the radiative feedback. Note that Figure 3.12 and Figure 3.13 have different x-axis scales. For Figure 3.12 CRH goes up to values higher than 90% while in Figure 3.13 CRH only goes up to values higher than 80%. This can be explained by the fact that there are no areas with high  $T_s$  that are very moist in the mid-troposphere.

The feedback binned by  $\text{CRH}_{1000}$  fluctuates around  $\lambda_{lw} = 1.75 \text{ W m}^{-2}$  until it starts to decrease for  $\text{CRH}_{1000} > 50\%$ . The feedback binned by  $\text{CRH}_{700}$  decreases nearly monotonically which suits my expectations and clearly shows the impact of mid-tropospheric CRH and the closing of the spectral window of water vapor on the radiative feedback.

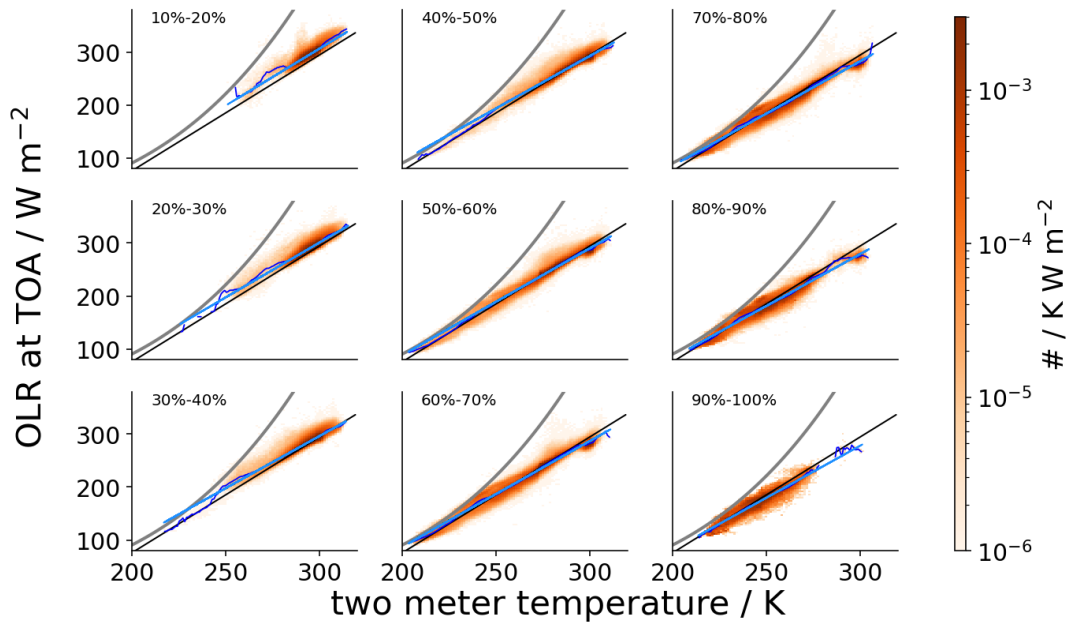


Figure 3.11: OLR (clear-sky CERES) dependence on  $T_s$  (all-sky ERA5) binned by  $CRH_{700}$ . The grey line indicates the Stefan-Boltzmann law (Equation 3.1), the black line indicates the mean radiative feedback ( $\lambda_{lw} = 2.175 \text{ W m}^{-2} \text{ K}^{-1}$ ), the light blue line indicates the feedback of every bin and the dark blue line indicates the mean OLR value for every  $T_s$  bin.

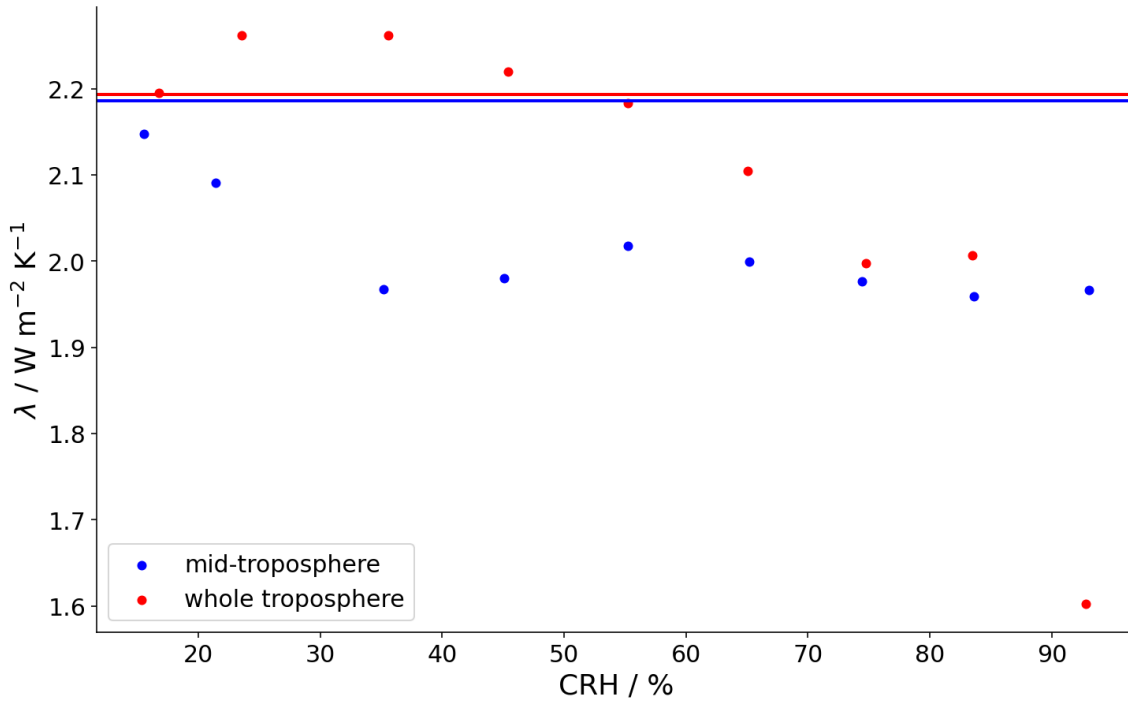


Figure 3.12: Feedback binned by  $CRH_{1000}$  (red) and by  $CRH_{700}$  (blue) for the whole  $T_s$  range.



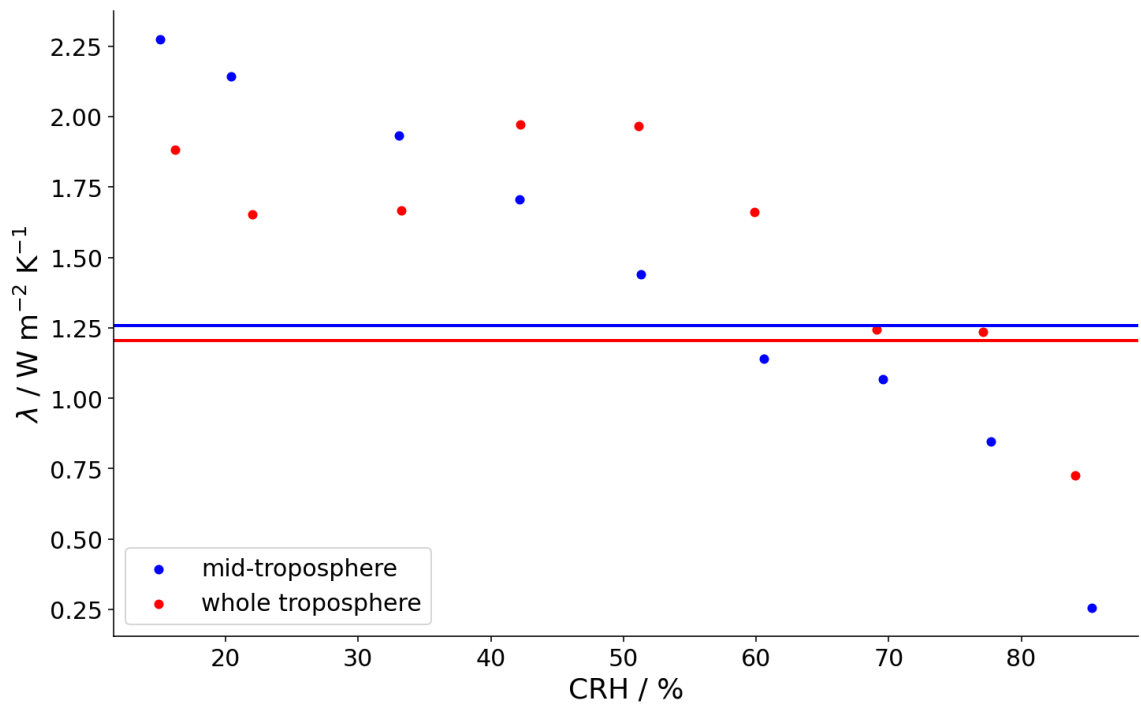


Figure 3.13: Feedback binned by  $\text{CRH}_{1000}$  (red) and by  $\text{CRH}_{700}$  (blue) for  $T_s > 290 \text{ K}$ .



## 4 Conclusion and Outlook

In this thesis, I investigated the impact of CRH on OLR. I focused on deviations from the linear relation between OLR and  $T_s$  by binning with CRH to analyze the effect of humidity. My results partly align with previous papers like [Koll and Cronin \[2018\]](#) and [McKim et al. \[2021\]](#).

I show that increasing CRH, hence closing the spectral window of water vapor, disrupts the linear relationship between OLR and  $T_s$  and causes the radiative feedback to decrease. This happens because OLR decreases more with increasing CRH than it increases with rising  $T_s$ . Thus, the atmosphere gets warmer because more radiation gets trapped by water vapor. A warmer atmosphere can host even more water vapor which means even less radiation gets through. This is when the super greenhouse effect has a striking impact on Earth's climate. My analysis shows that the linearity starts breaking down in tropical, warm, and moist areas. Furthermore, I found, that the impact of cloud cover coincides with [McKim et al. \[2021\]](#) as it shows an even stronger and smoother decrease of the feedback with CRH than for clear-sky data.

Nevertheless, some aspects do not meet my expectations. Even though the feedback decreases with increasing CRH, it decreases unmonotonically and less compared to [McKim et al. \[2021\]](#). The last part of my analysis revealed some unexpected results, too. The influence of mid-tropospheric CRH on the sudden decrease of OLR around 300 K is less than expected and shows only a slight increase of the bump around 300 K with increasing moisture in the mid-troposphere. [Feng \[2023\]](#) found that influence to be bigger. However, the analysis of mid-tropospheric CRH on the feedback shows that in the tropics the feedback is highly impacted by the mid-tropospheric CRH. It decreases monotonically with increasing mid-tropospheric CRH.

Nonetheless, my analysis shows the impact of rising water vapor content on the radiative feedback and the vicious circle as high water vapor content increases the temperature which leads to even more water vapor in the atmosphere.

To further verify both, expected and unexpected results, additional investigations are needed. Such as model-based analysis which would make my results more comparable to [Koll and Cronin \[2018\]](#) and [McKim et al. \[2021\]](#) as their analysis is based on models. Another way to improve my analysis might be to use data with higher vertical resolution to get better insights into the effect of different atmospheric layers. It would be easier to identify specific layers as the middle troposphere in [Chapter 3.3](#).



## Appendix

The  $CRH_{1000}$  distribution can be seen in Figure 4.1. It differs from the  $CRH_{700}$  distribution in Figure 4.2. It can be seen, that the areas north and south of the equator are drier in the mid-troposphere compared to the whole troposphere. Another noticeable aspect is that sand and ice deserts are not visible in the mid-tropospheric CRH but in the CRH of the whole troposphere.

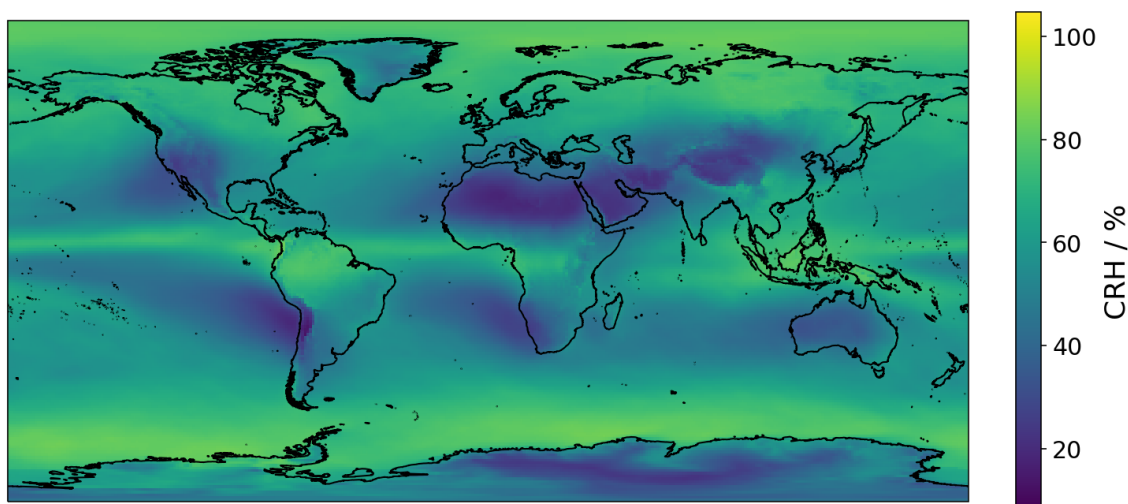


Figure 4.1: Yearly mean  $CRH_{1000}$  in 2022.

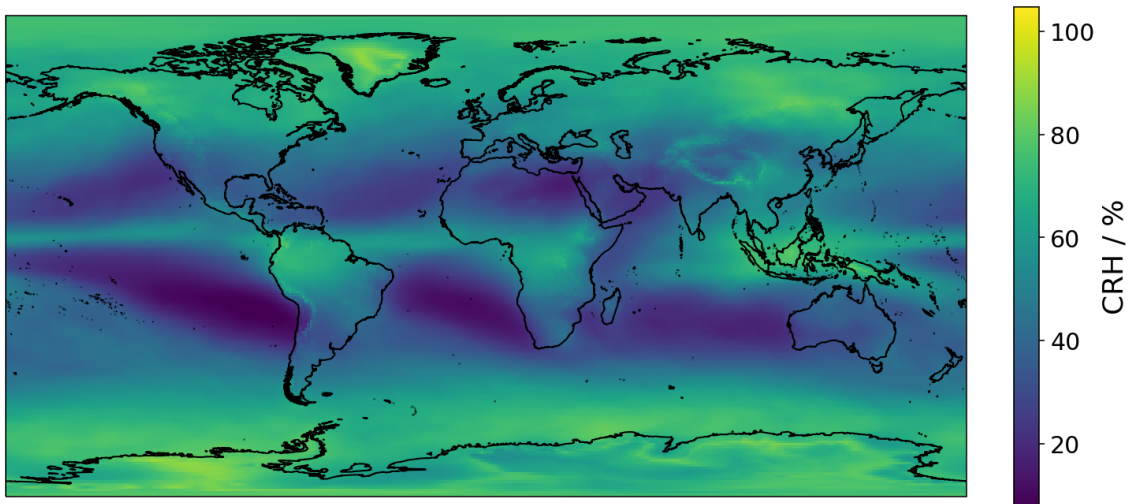


Figure 4.2: Yearly mean CRH<sub>700</sub> of 2022.

## Bibliography

- Daniel DB Koll and Timothy W Cronin. Earth's outgoing longwave radiation linear due to h<sub>2</sub>o greenhouse effect. *Proceedings of the National Academy of Sciences*, 115(41): 10293–10298, 2018.
- Brett A McKim, Nadir Jeevanjee, and Geoffrey K Vallis. Joint dependence of longwave feedback on surface temperature and relative humidity. *Geophysical Research Letters*, 48(18):e2021GL094074, 2021.
- Jing Feng. The importance of atmosphere on outgoing longwave radiation and longwave feedback. 2023.
- Stephanie S Rushley, Daehyun Kim, CS Bretherton, and M-S Ahn. Reexamining the non-linear moisture-precipitation relationship over the tropical oceans. *Geophysical research letters*, 45(2):1133–1140, 2018.
- NASA CERES. Ceres data products, 2022. URL <https://ceres.larc.nasa.gov/data/>.
- ERA5. Era5, 2022. URL <https://cds.climate.copernicus.eu/cdsapp#!/search?text=ERA5%20preliminary%20version&type=dataset>.
- Typhon. Typhon 0.9.0, 2023. <https://www.radiativetransfer.org/misc/typhon/doc/index.html>.
- DM Murphy and T Koop. Review of the vapour pressures of ice and supercooled water for atmospheric applications, *qj roy. meteor. soc.*, 131, 1539–1565, 2005.





# Acknowledgment

I want to thank my primary supervisor Prof. Dr. Stefan Bühler for the opportunity to write my thesis with him and for guiding me through the process of writing my thesis. I would also like to thank my second supervisor Florian Römer for his support and his patience. Whenever I had questions I could reach out to him no matter how basic my questions.

Furthermore, I would like to say thank you to my boyfriend Jon who was always there for me throughout the whole process and its ups and downs. Special thanks to him and Lennart for reviewing my thesis to help me improve the presentations of my results.

Not to forget, I want to thank my whole semester for the amazing past three years. Studying with you has been a lot of fun and even made the tough courses somehow enjoyable! I hope to continue with most of you during my masters! I also want thank to my friends on Svalbard for the mental support during the last weeks. Thanks for forcing me to take some breaks to free my mind!

Lastly, I would like to thank my parents Bernd and Birgit Nellesen for supporting me financially and mentally during the last years. Without your support this would not have been possible!



# Eidesstattliche Versicherung

Hiermit versichere ich an Eides statt, dass ich die vorliegende Arbeit im Studiengang Meteorologie selbstständig verfasst und keine anderen als die angegebenen Hilfsmittel – insbesondere keine im Quellenverzeichnis nicht benannten Internet-Quellen – benutzt habe. Alle Stellen, die wörtlich oder sinngemäß aus Veröffentlichungen entnommen wurden, sind als solche kenntlich gemacht. Ich versichere weiterhin, dass ich die Arbeit vorher nicht in einem anderen Prüfungsverfahren eingereicht habe und dass die gedruckte der elektronischen Fassung entspricht.

Einer Veröffentlichung der vorliegenden Arbeit in der zuständigen Fachbibliothek des Fachbereichs stimme ich zu.

Longyearbyen, den 19.09.2023

Unterschrift: \_\_\_\_\_

A handwritten signature in black ink, appearing to be 'L. N. B.', written over a horizontal line.